

On the origin of equatorial Atlantic biases in coupled general circulation models

Ingo Richter · Shang-Ping Xie

Received: 21 September 2007 / Accepted: 4 January 2008
© Springer-Verlag 2008

Abstract Many coupled ocean–atmosphere general circulation models (GCMs) suffer serious biases in the tropical Atlantic including a southward shift of the inter-tropical convergence zone (ITCZ) in the annual mean, a westerly bias in equatorial surface winds, and a failure to reproduce the eastern equatorial cold tongue in boreal summer. The present study examines an ensemble of coupled GCMs and their uncoupled atmospheric component to identify common sources of error. It is found that the westerly wind bias also exists in the atmospheric GCMs forced with observed sea surface temperature, but only in boreal spring. During this time sea-level pressure is anomalously high (low) in the western (eastern) equatorial Atlantic, which appears to be related to deficient (excessive) precipitation over tropical South America (Africa). In coupled simulations, this westerly bias leads to a deepening of the thermocline in the east, which prevents the equatorial cold tongue from developing in boreal summer. Thus reducing atmospheric model errors during boreal spring may lead to improved coupled simulations of tropical Atlantic climate.

1 Introduction

Tropical Atlantic climate displays large east-west and north-south asymmetries, with a cold tongue developing from the coast of southern Africa toward the west along the equator, and a zonal band of high sea surface temperature (SST) north of the equator that anchors the intertropical convergence zone (ITCZ). The southeast trade winds prevail on the equator year-round, colliding with the northeast trades along the ITCZ. During boreal summer, these asymmetries are most pronounced while during spring, the SST field is nearly symmetrical about the equator with uniformly warm SST covering the entire equatorial Atlantic. The influence of adjacent continents is evident: in May, strong southerly surface winds in the Gulf of Guinea associated with the onset of the West African monsoon are instrumental in initiating the seasonal development of the equatorial cold tongue, by inducing upwelling along the southern African coast and in the open ocean just south of the equator (Mitchell and Wallace 1992; Okumura and Xie 2004).

The realistic simulation of tropical Atlantic climate remains a challenge for state-of-the-art coupled ocean–atmosphere general circulation models (GCMs). Most models fail to reproduce the observed eastern equatorial cold tongue in boreal summer, and many even place cool SSTs in the western basin where a warm pool is observed in nature. In the annual mean this is manifested as a reversal of the climatological SST gradient along the equator as shown in an earlier coupled model intercomparison by Davey et al. (2002). Despite substantial model development in the intervening years, the basic problem remains in coupled GCMs, such as those participating in the Intergovernmental Panel on Climate Change (IPCC) Fourth Assessment Report (AR4). Figure 1 compares

I. Richter (✉) · S.-P. Xie
International Pacific Research Center,
University of Hawaii at Manoa,
2525 Correa Road, Honolulu,
HI 96822, USA
e-mail: irichter@hawaii.edu

S.-P. Xie
Department of Meteorology,
University of Hawaii at Manoa,
Honolulu, HI, USA

June–July–August (JJA) SST in simulations and observations, with the former represented by an AR4 multi-model ensemble mean from their Climate of the 20th Century runs. It is obvious from Fig. 1 that the models fail to capture the cold tongue in the eastern equatorial Atlantic; instead, relatively cool SSTs are found in the western equatorial Atlantic. This constitutes a reversal of the climatological SST gradient as reported by Davey et al. (2002). Furthermore, coupled models produce too much precipitation south of the equator during March–April–May (MAM), which leads to a spurious double-ITCZ in the annual mean (Breugem et al. 2006; Deser et al. 2006; Stockdale et al. 2006). This double-ITCZ syndrome also

persists in coupled simulations of the tropical Pacific climate (Mechoso et al. 1995; de Szoeke and Xie 2008).

In addition to the warm bias in the eastern equatorial region, Fig. 1 shows an even more pronounced warm bias to the south along the coast of Southwest Africa. This type of error is also seen in the southeast Pacific and is likely due to the under-representation of stratocumulus and coastal upwelling (Ma et al. 1996; Large and Danabasoglu 2006; Huang et al. 2007). The southeast Atlantic bias also features prominently in seasonal forecast models that do not suffer from serious equatorial biases, such as the NCEP Coupled Forecast System (CFS; Huang et al. 2007), suggesting that the two types of biases may be distinct in their origins.

Since modes of tropical Atlantic variability involve ocean–atmospheric feedbacks that are dependent on the mean state (Xie and Carton 2004; Chang et al. 2006; Kenyanside and Latif 2007), the failure of coupled GCMs to simulate a realistic mean state bodes ill for their ability to predict seasonal-to-interannual SST and precipitation anomalies (Repelli and Nobre 2004; Stockdale et al. 2006). It also calls into question the credibility of long-term projections for the region under climate forcing scenarios (Breugem et al. 2006). It is therefore important to investigate the causes of GCM biases in the tropical Atlantic and to work toward their elimination.

While coupled ocean–atmosphere feedbacks certainly play a role in producing the above biases, previous studies have shown that even uncoupled atmospheric GCMs (AGCMs) with prescribed climatological SSTs suffer significant biases. Biasutti et al. (2006) find that the southward shift of the ITCZ is a common problem in atmospheric GCMs and that it is often accompanied by a tendency to place the rainfall over the SST maximum whereas observations place it over the surface convergence maximum. Chang et al. (2007) show that the National Center for Atmospheric Research (NCAR) Community Atmospheric Model (CAM) underestimates the equatorial easterlies, contributing significantly to the biases when coupled with an ocean GCM (see also DeWitt 2005). Richter et al. (2008) show that atmospheric GCM precipitation biases over tropical South America and Africa have the potential to affect the simulation of the South Atlantic anticyclone. In a coupled model such biases in the southeast trades force an SST response, leading to basin-wide adjustments in the ocean and atmosphere through the wind–evaporation–SST (WES) feedback (Xie 1996).

The present study investigates the sources of coupled model biases over the equatorial Atlantic, with a focus on the lack of the eastern cold tongue on the equator and the double ITCZ in the models. In particular, we explore the hypothesis that the surface wind and precipitation biases in coupled GCMs originate in their atmospheric component

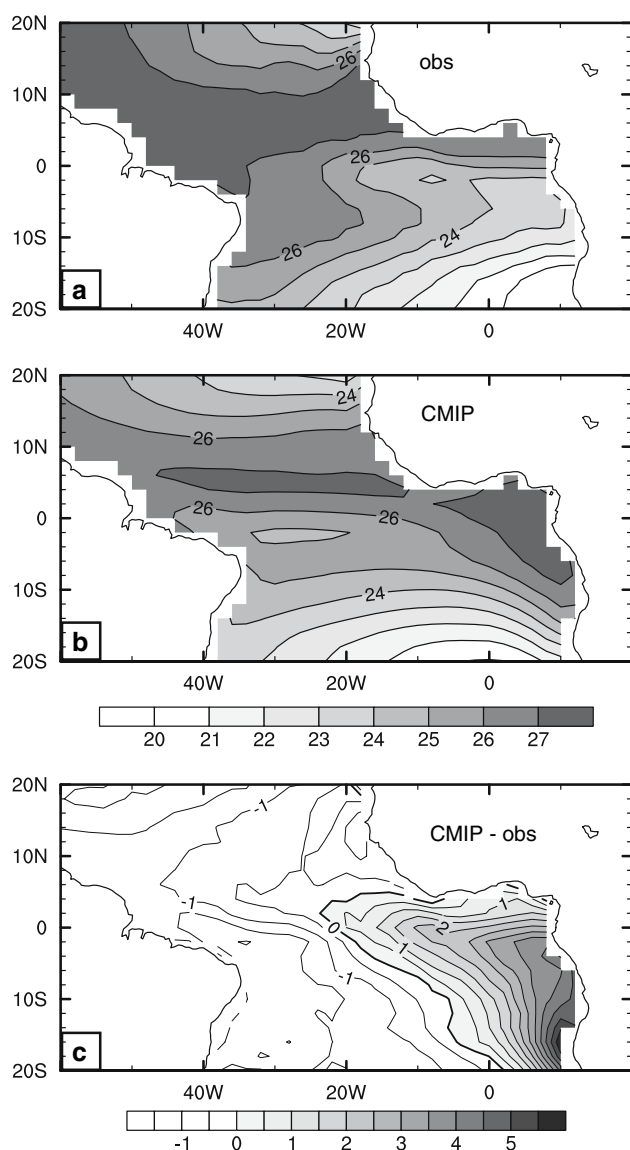


Fig. 1 JJA SST (°C) for **a** ICOADS observations, **b** the CMIP model ensemble-mean, and **c** the difference **b** – **a**. Shading in the difference plot (c) indicates positive values

and are amplified by coupled ocean–atmosphere feedbacks. This hypothesis is tested by comparing several pairs of coupled and atmosphere-only GCM simulations performed for the IPCC AR4. Our objectives are to (1) identify common problems in the coupled GCMs, and (2) examine to what extent these errors can be traced back to shortcomings in the atmospheric component.

While several studies have addressed tropical Atlantic biases, our approach is unique in its utilization of a multi-model database that includes both coupled GCMs and their atmospheric component. This allows us to identify common error patterns, their atmospheric sources, and their amplification by coupled processes. Furthermore, while most studies have focused on the annual mean or boreal summer, our study examines the seasonal evolution of errors and identifies MAM as the crucial season.

The rest of the paper is organized as follows. Section 2 introduces the models and their simulations. In Sects. 3 and 4 we analyze the models' simulation of the equatorial cold tongue and meridional asymmetry, respectively. Section 5 gives the summary of our results and discusses general implications.

2 Models

We examine IPCC AR4 Climate of the 20th Century (also known as the Coupled Model Intercomparison Project or CMIP-3) integrations and the simulations by their atmospheric component. In the atmosphere-only runs, the atmospheric GCMs are forced with observed SSTs, following the Atmospheric Model Intercomparison Project (AMIP) protocols. Monthly climatologies are obtained using years 1950–1999 (CMIP) and 1979–1999 (AMIP), the latter being the maximum common period for the AMIP simulations. The description of individual models is available at http://www-pcmdi.llnl.gov/ipcc/model_documentation/ipcc_model_documentation.php (see also Meehl et al. 2005).

All model output was interpolated to a $2^\circ \times 2^\circ$ grid. Ensemble means for CMIP and AMIP simulations were calculated from the six models marked by asterisks in Table 1, all developed at major modeling centers. Requiring AMIP simulations in the AR4 database reduces the number of models for analysis significantly. However, the composites shown here are very similar if a larger set of CMIP models is selected. Thus our ensemble average using a subset represents well the typical biases in the coupled AR4 GCMs.

The following observational datasets are used for comparison: Climate Prediction Center (CPC) Merged Analysis of Precipitation (CMAP; Xie and Arkin 1997); International Comprehensive Ocean Atmosphere Dataset

Table 1 Summary of models considered in this study and the labels used to denote them in legends and scatter plots

| Model/dataset | Label | Model/dataset | Label |
|------------------|-------|------------------|-------|
| Obs | a | mpi_echam5* | l |
| Reanalysis | b | ncar_ccsm3_0* | m |
| Ensemble | c | ukmo_hadcm3 | n |
| Cnrm_cm3* | d | ukmo_hadgem1* | o |
| Csiro_mk3_0 | e | bccr_bcm2_0 | p |
| gfdl_cm2_0 | f | giss_aom | q |
| gfdl_cm2_1 | g | giss_model_e_h | r |
| Ingv_echam4 | h | giss_model_e_r | s |
| ipsl_cm4 | i | iap_fggoals1_0_g | t |
| miroc3_2_hires* | j | miub_echo_g | u |
| miroc3_2_medres* | k | ncar_pcm1 | v |

The asterisk marks models that are part of the AMIP and CMIP ensemble means

(ICOADS; Worley et al. 2005) for SST, surface winds and sea level pressure; International Satellite Cloud Climatology Project (ISCCP; Rossow and Schiffer 1999) for net surface shortwave radiation; National Center for Environmental Prediction (NCEP) reanalysis (Kalnay et al. 1996) for latent heat flux; and National Oceanographic Data Center (NODC) World Ocean Atlas (WOA; Conkright et al. 2002) for the computation of the 20°C isotherm depth.

3 Zonal biases

Figure 2 shows annual mean SSTs along the equator for 12 CMIP models. The spread is considerable with a mean temperature difference among models of up to 3 K (UKMO HadCM3 vs. CNRM CM3). Common to all models, however, are (1) a reversed temperature gradient in the central Atlantic, and (2) a warm bias in the east (with the exception of the CNRM model, which suffers from a general cold bias along the equator). In general, the deficiencies are similar to those shown in Davey et al. (2002), albeit slightly less severe.

The ensemble mean seasonal evolution of SST and surface wind biases along the equator is depicted in Fig. 3a. During MAM a strong westerly bias appears in the central and eastern equatorial Atlantic. This is accompanied by a weak warm (cold) SST bias in the east (west). In the following season the westerly bias relaxes while the SST bias grows to maximum strength, with the error in east-west SST difference reaching $\sim 4\text{K}$ during July–August. In contrast to the observed eastern cold tongue, the modeled SST along the equator increases toward the east (Fig. 1).

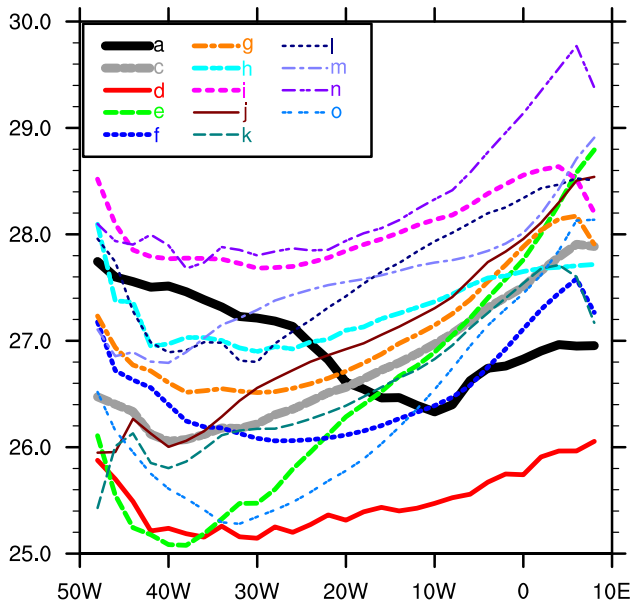


Fig. 2 Annual mean of SST (°C) along the equator in selected CMIP models averaged between 2°S and 2°N. The *thick black and gray lines* show ICOADS observations and the ensemble mean, respectively

In search for the source of the coupled model biases, we turn to the AMIP simulations. Figure 3b shows the seasonal evolution of ensemble mean errors in surface wind and precipitation along the equator. The figure clearly documents that the westerly bias is already present in the uncoupled GCMs, albeit somewhat weaker. In contrast to CMIP, however, the westerly bias only exists from February to May, when it is accompanied by a positive sea-level pressure bias in the western equatorial Atlantic (Fig. 3c). This sea level pressure error can be further traced back to the east-west contrast in precipitation. As Fig. 3b shows, east-west precipitation errors occur during approximately the same period as the westerly bias but appear one month earlier. Equatorial precipitation is underpredicted in the west, off the South American coast, and overpredicted in the east, off the African coast. Figure 4b shows the precipitation errors in the AMIP ensemble during MAM, which are characterized by a meridional dipole over the ocean (which will be discussed in detail in Sect. 4) that is slightly tilted and thus gives rise to a zonal component in

the equatorial Atlantic biases. These precipitation biases are not confined to the ocean but extend to the adjacent continents. In particular, simulated rainfall is deficient over equatorial South America and excessive over equatorial

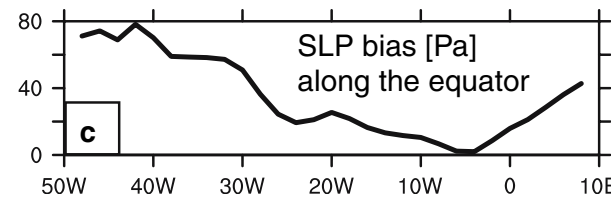
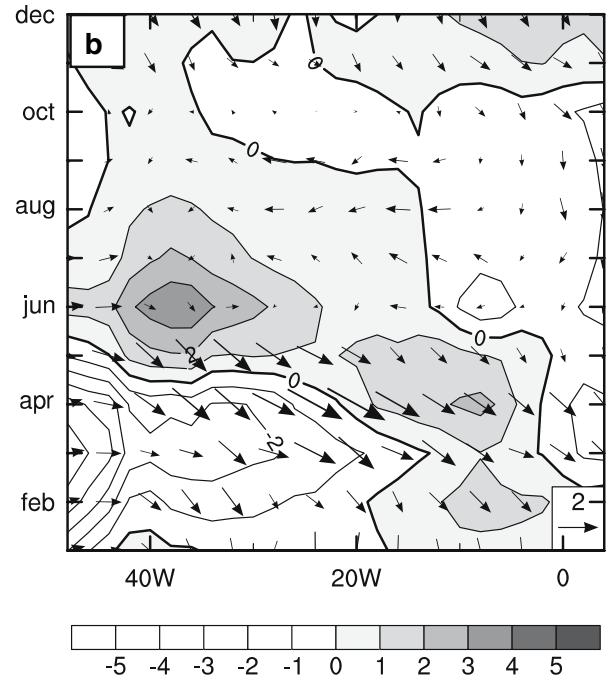
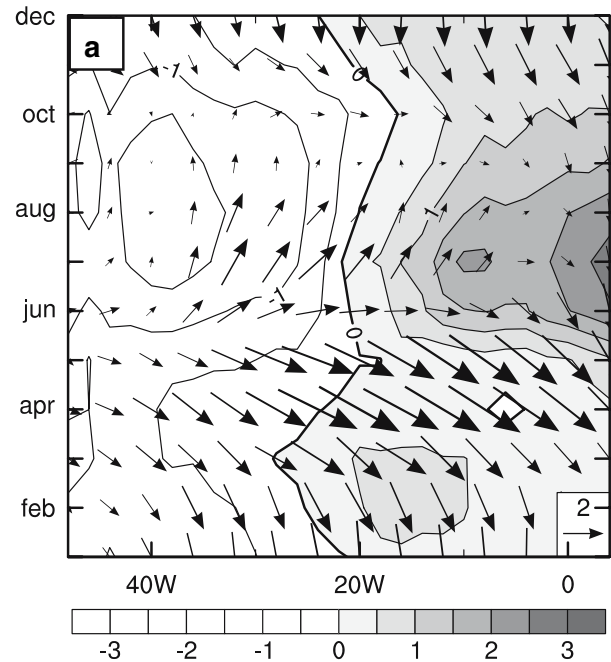
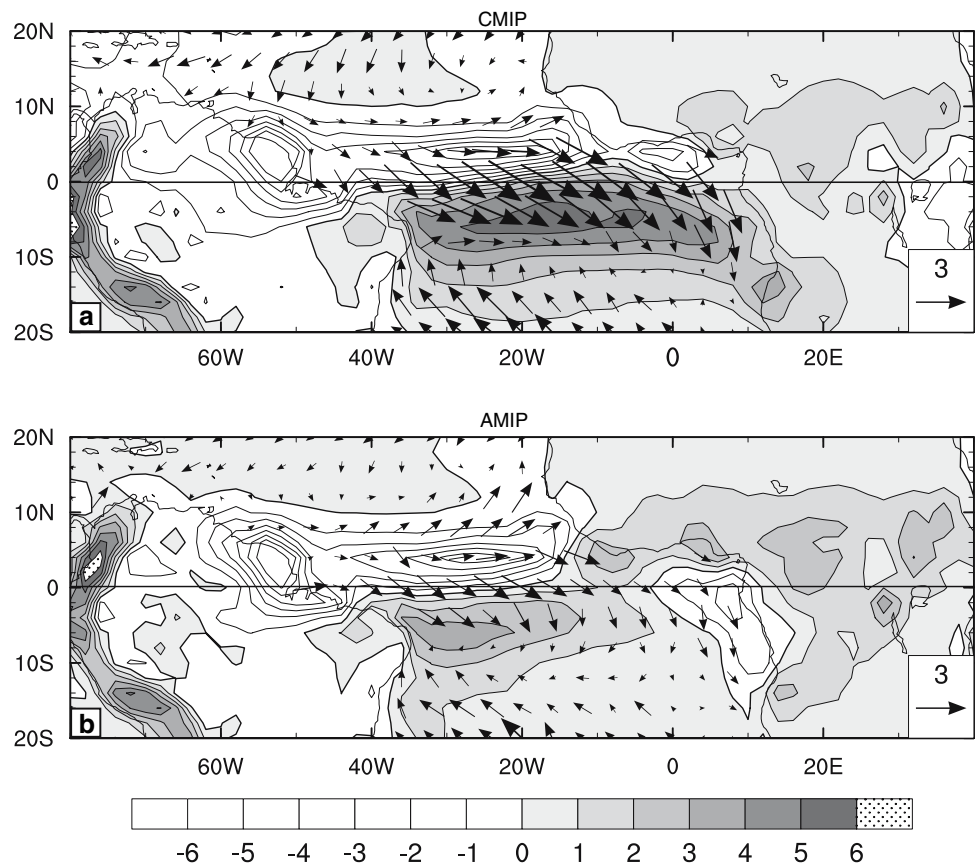


Fig. 3 **a** Longitude-time sections of surface winds (m/s, vectors) and SST biases (°C, contours) in CMIP. **b** Biases of surface winds (m/s, vectors) and precipitation (mm/day, contours) in AMIP. **c** Bias of sea level pressure (Pa) along the equator during MAM in AMIP. All fields are meridionally averaged between 2°S and 2°N. Positive values in **a** and **b** are shaded. Model biases are in reference to ICOADS (SST and surface winds) and CMAP (precipitation). The fields shown represent the ensemble mean over selected CMIP models (**a**) and AMIP models (**b**, **c**). The ensemble members are indicated in Table 1

Fig. 4 MAM precipitation (mm/day, contours; *positive shaded*) and surface wind (m/s, vectors) biases for **a** CMIP, and **b** AMIP ensemble means. The reference data for precipitation and winds are CMAP and ICOADS, respectively



Africa. This east-west dipole of precipitation errors drives the westerly wind biases over the equatorial Atlantic. Such precipitation and wind errors are consistent with a weakened Atlantic Walker cell as reported for the CAM 3 by Chang et al. (2007). Okumura and Xie (2004) also note the westerly bias in equatorial winds during the warm season in an atmospheric GCM.

While the westerly bias in both AMIP and CMIP models peaks during MAM, the SST error is most pronounced from June to September. This delayed SST response can be explained as follows. The westerly wind error during MAM causes the thermocline to deepen in the east (Fig. 5). The deepening peaks in May with values in excess of 30 m. In the following season, the westerly bias weakens while the cross-equatorial southerly winds, which are crucial to equatorial upwelling (e.g., Okumura and Xie 2004), are even slightly stronger than observed. Thus the wind patterns would be otherwise favorable for upwelling and cold tongue development, but the unrealistically deep thermocline prevents equatorial Atlantic cooling, resulting in a peak in the warm SST bias during the observed cold tongue season (JJA).

With the equatorial westerly bias weakening, the thermocline depth slowly recovers from June and reaches approximately the observed values in September. In the full

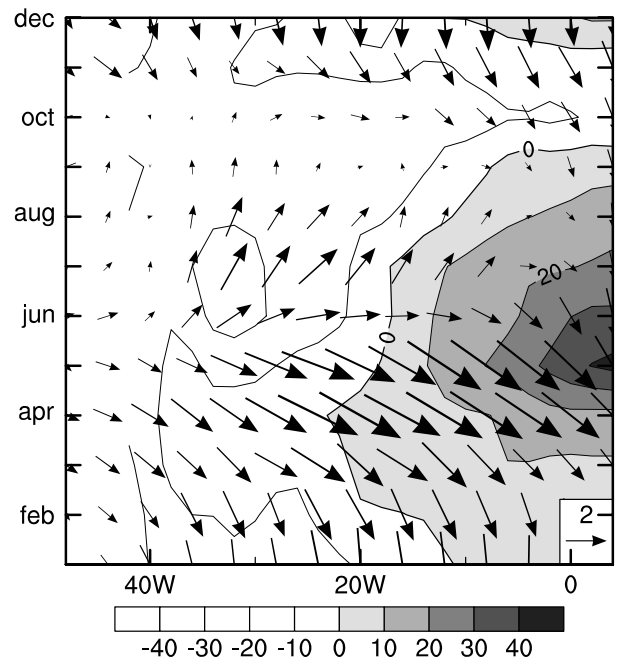


Fig. 5 Longitude-time sections of the CMIP ensemble-mean biases of surface wind (m/s, vectors) and the 20°C isotherm depth (m, contours). The reference datasets are ICOADS (surface winds) and NODC WOA (isotherm depth)

fields (Fig. 6a), the model thermocline begins with too large a depth (90 m in the east) in May and never becomes as shallow as in observations: the minimum 20°C-isotherm depth is less than 40 m in observations (July) but 50 m in the model ensemble (September). The southerly winds in the Gulf of Guinea begin to weaken in September as the West African monsoon begins its withdrawal. As a result of the excessively deep thermocline, the boreal summer cooling in the Gulf of Guinea (Fig. 6b) is much subdued in the models, reaching a minimum SST of 26.5 rather than the observed 24.5°C. In observations, the thermocline shoals again in the eastern equatorial Atlantic in December because the secondary acceleration of the equatorial easterly winds excites the resonant basin mode of equatorial ocean wave adjustment (Okumura and Xie 2006; Helber et al. 2007). The models underestimate this December shoaling of the thermocline.

Figure 7 illustrates the relationship between MAM surface zonal wind (averaged between 2°S–2°N and 40°W–10°W) and JJA SST gradient (difference between 40°W and 8°E, averaged 2°S–2°N) among 19 CMIP models. The inter-model correlation is 0.76. A similar analysis for the zonal wind bias in April–May and anomalous thermocline depth gradient in May–June yields a correlation of 0.89. These correlations suggest that in the coupled models studied here, there is a close link between MAM westerly errors, the erroneously deep thermocline in the east, and the failure to develop an equatorial cold tongue in boreal summer.

The correlations also indicate that the Bjerknes feedback plays a role in the development of the large SST biases during JJA. We isolate this coupled feedback by calculating the CMIP–AMIP difference in atmospheric fields, which represents the atmospheric response to CMIP SST biases. Note that CMIP SST biases result from AMIP atmospheric biases as well as this CMIP–AMIP difference. Figure 8b shows SST errors, and the CMIP–AMIP differences in precipitation and surface wind. In the equatorial Atlantic, the eastern warming and western cooling induce westerly wind anomalies, which is indicative of the Bjerknes feedback. The eastern warming is partially due to the deepened thermocline in response to MAM westerly wind biases while the SST-induced westerly anomalies help deepen the thermocline even more in the east.

4 Meridional biases

In addition to the zonal biases discussed so far, the AMIP models also feature the well-known southward shift of the ITCZ (Huang et al. 2004; Biasutti et al. 2006). Figure 4 shows surface winds and precipitation during MAM, the season when the observed ITCZ reaches its southernmost

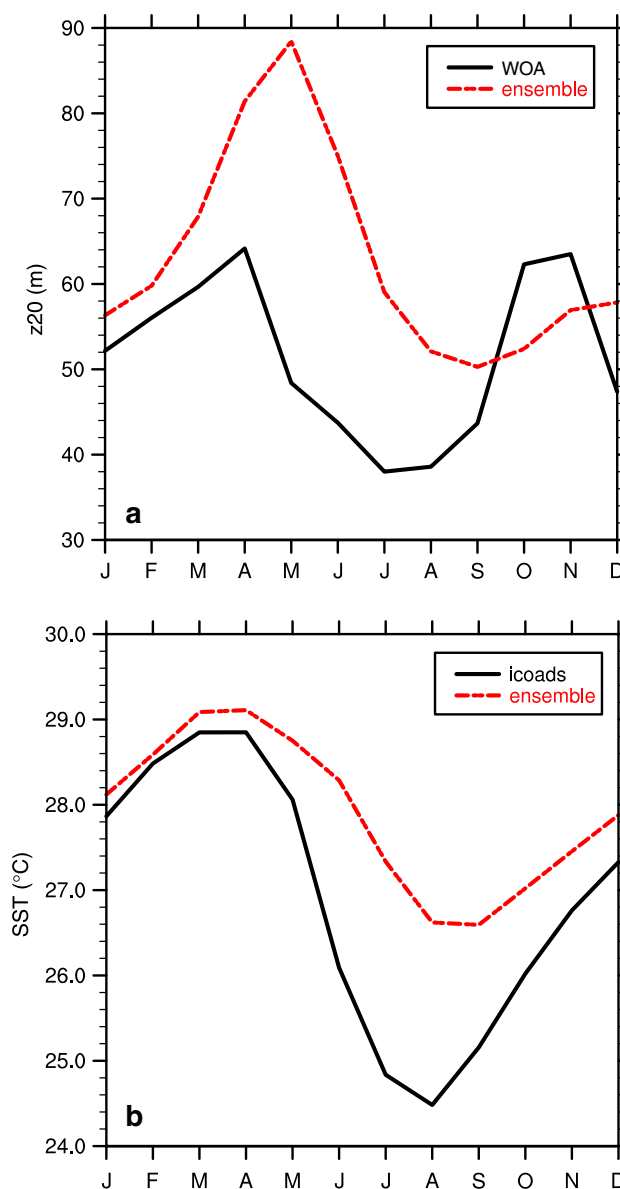


Fig. 6 Annual cycles in the eastern equatorial Atlantic (0°–5°E, 2°S–2°N) of **a** depth of the 20°C isotherm, and **b** SST. The *solid and dashed lines* denote observations and model ensemble, respectively. The observations are World Ocean Atlas for isotherm depth and ICOADS for SST

position in the Atlantic, and sometimes migrates south of the equator. The coupled GCMs place the Atlantic ITCZ south of the equator and thus overpredict rainfall there, in association with a northerly error in cross-equatorial winds. As with the zonal biases, these errors exist, to a large extent, in both the CMIP (Fig. 4a) and AMIP (Fig. 4b) simulations but are more pronounced in the former. It is interesting to note that the southward shift of precipitation is limited to the western equatorial Atlantic in AMIP but extends across the basin in CMIP, suggestive of SST effects in the latter.

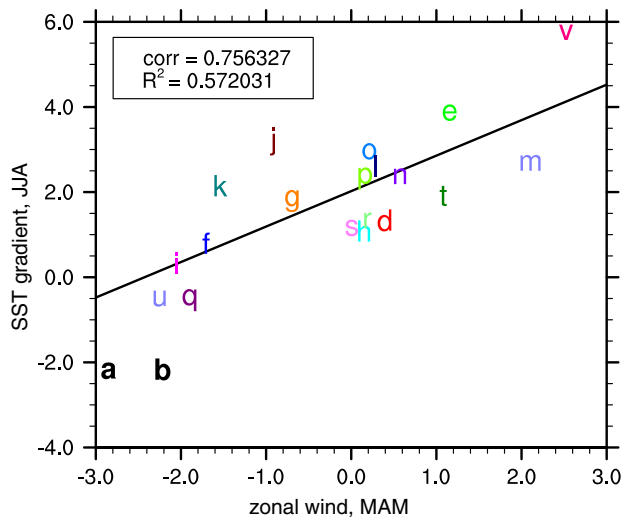


Fig. 7 Scattering among CMIP models of MAM zonal surface wind (m/s; averaged between 2°S–2°N and 40–10°W), and JJA SST gradient between 40°W and 8°E (K; averaged between 2°S and 2°N). Model labels are listed in Table 1

We further examine the coupled feedbacks in Fig. 8a, which shows the CMIP–AMIP difference in surface winds and precipitation. The warm SST biases are confined to the Southeast Atlantic and peak off the southern African coast (20°S) possibly because of the depressed thermocline that results from the equatorial westerly bias via equatorial and coastal Kelvin waves. The SST error pattern resembles the Benguela Niño that tends to peak during MAM in observations (Shannon et al. 1986; Rouault et al. 2003). SST errors are small on the equator during MAM because upwelling does not play an important role during this season, thus reducing the impact of simulated errors in thermocline depth and cross-equatorial winds. The warm SST errors in the Southeast Atlantic amplify errors in the atmospheric fields by enhancing the spurious southern ITCZ rain band and by increasing northeasterly wind errors near the equator. The CMIP–AMIP wind difference is much stronger south than north of the equator, and the weakened southeasterly winds south of the equator act to reduce surface evaporation and warm the SST there, indicative of the WES feedback. The CMIP–AMIP northwesterly wind difference on the equator might also help maintain the SST warming in the Southeast Atlantic by deepening the thermocline in the Benguela coastal region. From January to June, the WES and thermocline feedbacks are necessary to overcome the reduced solar radiation due to increased convective clouds and sustain the SST warming just south of the equator (Fig. 9). During July–December, on the other hand, the shortwave feedback turns positive over the SE Atlantic because the erroneously warm SST inhibits the formation of low-level clouds,

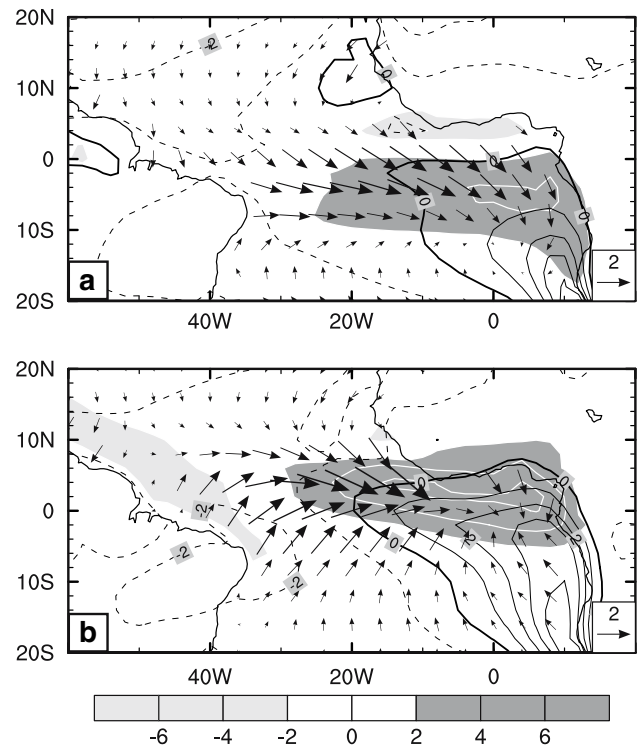


Fig. 8 Difference of the CMIP and AMIP ensemble means of surface winds (m/s, vectors), and precipitation (mm/day, shading and white contours), and SST (°C, contours) for **a** MAM, and **b** JJA. Precipitation differences less than –2 mm/day and greater than +2 mm/day are shaded light and dark gray, respectively. The interval for the white precipitation contours is 2 mm/day, the interval for the black SST contours is 1°C. Negative SST contours are dashed

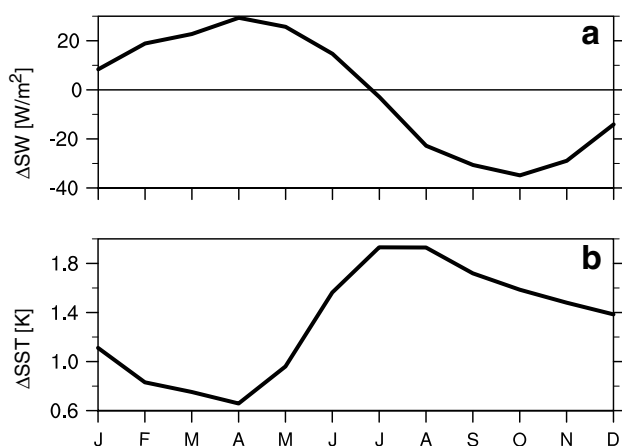
which are observed to prevail during this season (Klein and Hartmann 1993).

Figure 10 examines the amplification of the MAM northwesterly wind error on the equator in individual CMIP models. The MAM surface wind errors are averaged over the area 40–10°W and 2°S–2°N for both AMIP and CMIP runs. In all the models the westerly bias (Fig. 10a) becomes more severe in the coupled simulations, consistent with the Bjerknes feedback. The strength of this feedback, however, varies greatly from model to model, with the strongest response in the NCAR PCM, and the weakest in the GISS model. These differences are probably related to the mean thermocline depth, which is shallow in the former but very deep in the latter model (not shown).

The meridional wind biases for the same region (Fig. 10b) show a similar pattern. The majority of the models feature an increase of the northerly bias in their CMIP runs relative to their AMIP runs but there are several exceptions, namely the IPSL model, MIROC high and low resolution models, and the GISS model. All of these models also happen to feature a relatively small zonal wind bias in their CMIP runs. The amplification of the zonal and meridional surface wind biases is summarized in Table 2.

Table 2 Zonal (u) and meridional (v) surface wind velocity biases (m/s) in AMIP and CMIP ensembles for MAM, averaged over 40°W–10°W and 2°S–2°N. Biases are in reference to ICOADS

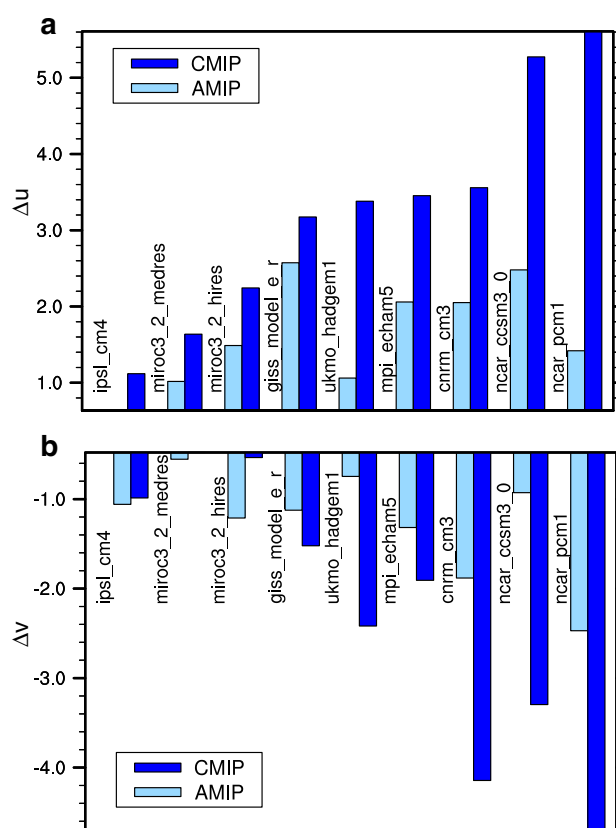
| Ensemble | Δu | Δv |
|----------|------------|------------|
| AMIP | 1.36 | −1.07 |
| CMIP | 2.69 | −2.07 |

**Fig. 9** Seasonal cycle in the SE Atlantic (10°W–10°E, EQ–20°S), for CMIP biases of **a** net surface shortwave radiation (W/m^2 , downward positive), and **b** SST (K). The reference datasets are ISCCP (shortwave) and ICOADS (SST)

Atmospheric error patterns differ between MAM and JJA in their meridional structure. In MAM, the warm SST bias, and the precipitation and wind errors are all located south of the equator while in JJA, wind and precipitation biases are maximum on the equator (Fig. 8). These differences in meridional structure may reflect the dominant modes of climate variability: the meridional mode and Benguela Niño tend to occur during MAM while the Atlantic Niño dominates JJA in observations (Xie and Caton 2004). The latter is due to the seasonal shoaling of the thermocline in the eastern equatorial Atlantic.

5 Continental precipitation biases

Our AMIP analysis in Sect. 3 suggests that the dipole of rainfall deficit over equatorial South America and excess over tropical Africa sets up a pressure gradient that drives the westerly wind biases in the equatorial Atlantic. While major re-organization of precipitation takes place over the ocean in CMIP, CMIP–AMIP precipitation differences induced by SST errors are small over land, generally less than 1 mm/day in magnitude (Fig. 8) except on the coast of Guinea. Thus it appears that errors in continental convection induce errors in simulated Atlantic climate but not the other way around.

**Fig. 10** Bar charts of surface wind biases in individual models averaged between 40 and 10°W for **a** zonal winds, and **b** meridional winds. The light and dark bars represent AMIP and CMIP models, respectively. The corresponding model names are displayed next to the bars

The seasonal evolution of continental precipitation biases in AMIP is depicted in Figs. 11 and 12 as longitude- and latitude-time sections, respectively. On the equator, deficient rainfall over South America develops from January to August and is pronounced during March and April between 60 and 40°W, coinciding with the rainy season there (Fig. 11a, c). During this period precipitation in the AMIP ensemble mean is underestimated by approximately 50%, indicative of systematic model deficiencies in representing convection in the region. The seasonality of the South American precipitation biases is further illustrated by latitude-time sections (Fig. 12). While the observed South American ITCZ migrates northward from January to July following the seasonal march of insolation (Fig. 12a), the model rainfall biases are stationary and confined to the equator and slightly north of it (Fig. 12c).

The center of the deficient precipitation in MAM is located just inland of the equatorial South American coast (Fig. 4b), which coincides with the observed precipitation maximum (not shown). The origin of this precipitation maximum has not received much attention but the few

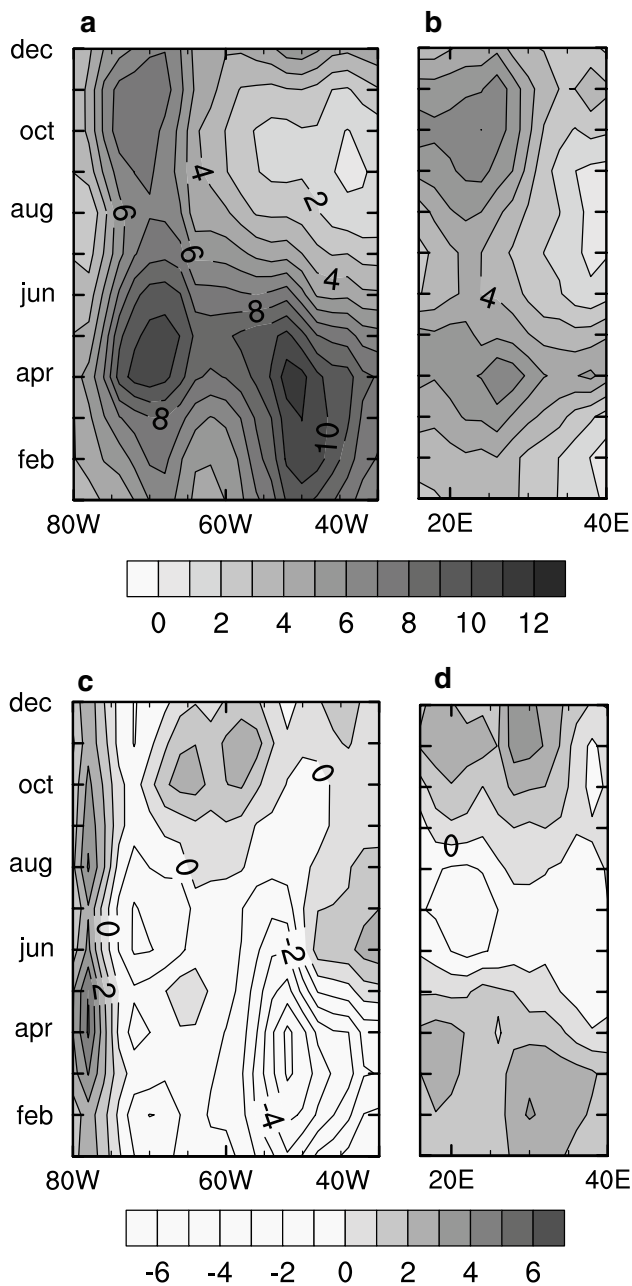


Fig. 11 Longitude-time sections of continental precipitation (mm/day) over equatorial South America (a, c) and Africa (b, d). The upper panels show CMAP observations, the lower panels the bias of the AMIP ensemble mean. Fields are averaged between 5°S and 5°N. Positive values in c and d are shaded

studies available point to the importance of mesoscale processes (Kousky 1980; Cohen et al. 1995; Rickenbach 2004). Specifically the interaction of the local sea breeze system and orography with the northeast trade winds during MAM is believed to generate mesoscale convective systems that propagate further inland and produce precipitation over a wide area. Typical AGCM resolutions at 2–3° are too coarse to capture such processes and this

might be one of the reasons for the deficient precipitation over equatorial South America.

Another feature of interest in Fig. 11c is the excessive precipitation over the Andes, which persists throughout the year. Such biases associated with steep orography are well known and likely related to the formulation of the pressure gradient force in sigma coordinates (e.g., Mesinger et al. 1988). The spurious convection generated over the mountains excites gravity waves that can potentially affect precipitation in the surrounding region but whether this contributes to the bias in equatorial South America is not clear.

Over equatorial Africa the observed seasonal cycle of precipitation (Fig. 11b) features two maxima during boreal spring and fall consistent with insolation. The AMIP simulations exaggerate this seasonal cycle, producing too much precipitation during spring and fall, and too little during summer (Fig. 11d). The magnitude of the bias, however, does not exceed 3 mm/day and is thus substantially smaller than over South America. The latitude-time sections (Fig. 12b, d) show a similar exaggeration of the seasonal cycle in precipitation. While the AMIP models track the seasonal migration of the ITCZ quite well, they overestimate its strength by 1–3 mm/day.

While part of the continental biases might be attributable to the models' shortcomings in simulating convection, the misrepresentation of land surface processes may also contribute to the errors. For example, comparison with the NCEP reanalysis suggests that the AMIP runs underestimate latent heat flux everywhere in South America, with differences exceeding 20 Wm^{-2} in equatorial South America, where the maximum rainfall deficit exists (Fig. 13). The situation is more complex in tropical Africa where there are positive and negative latent heat flux differences in the Sahel and equatorial Africa, respectively, while precipitation differences are positive in both regions. Since there are few observations of latent heat flux in these regions of interest, we do not have a solid reference to judge the models' performance. At least for South America, however, the comparison with NCEP does hint at a potential problem in the simulation of land surface processes. This begs the question whether there are any common deficiencies in the land surface parameterizations of the models examined here. While the land surface models employed vary substantially in their degree of sophistication, their basic formulations share many common features: calculation of surface turbulent fluxes through the aerodynamic bulk formula, a surface energy balance that includes ground heat flux, and a surface water balance that includes the contributions from precipitation, runoff, infiltration, and evaporation. The IPCC model archive, however, does not provide sufficient data to evaluate land surface parameters, and neither is there sufficient observational data to validate

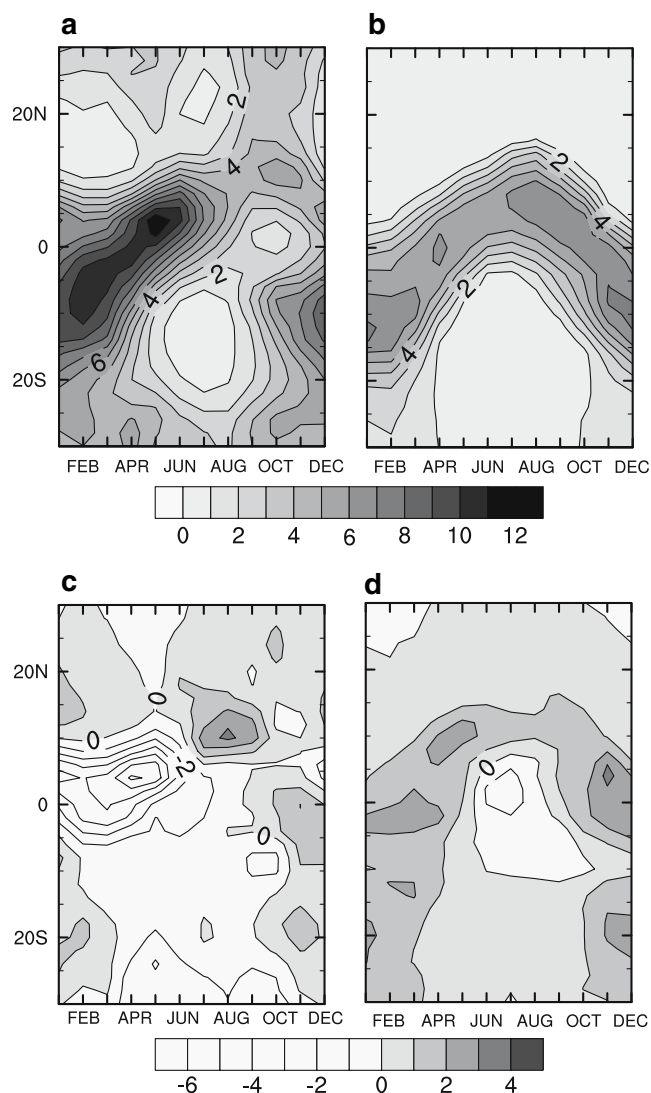


Fig. 12 Latitude time sections of continental precipitation (mm/day) over equatorial South America (**a**, **c**) and Africa (**b**, **d**). Averaging longitudes are 60–50°W (South America) and 15–30°E (Africa). The *upper panels* show CMAP observations, the *lower panels* the bias of the AMIP ensemble mean. Positive values in **c** and **d** are shaded

them against (see Dirmeyer et al. 2006). Potential deficiencies in the land surface parameterizations are therefore left as a topic of future studies.

In view of several previous studies, it might not come as a surprise that continental convection exerts a strong influence on the climate of a small ocean basin like the Atlantic. The rapid SST cooling in the Gulf of Guinea from May to July has been attributed to the abrupt onset of West African monsoon and southerly cross-equatorial winds (Mitchell and Wallace 1992; Okumura and Xie 2004). Recent results suggest that precipitation over land affects the latitudinal position of the ITCZ (Wang and Fu 2007; Hagos and Cook 2005). Richter et al. (2008) show that

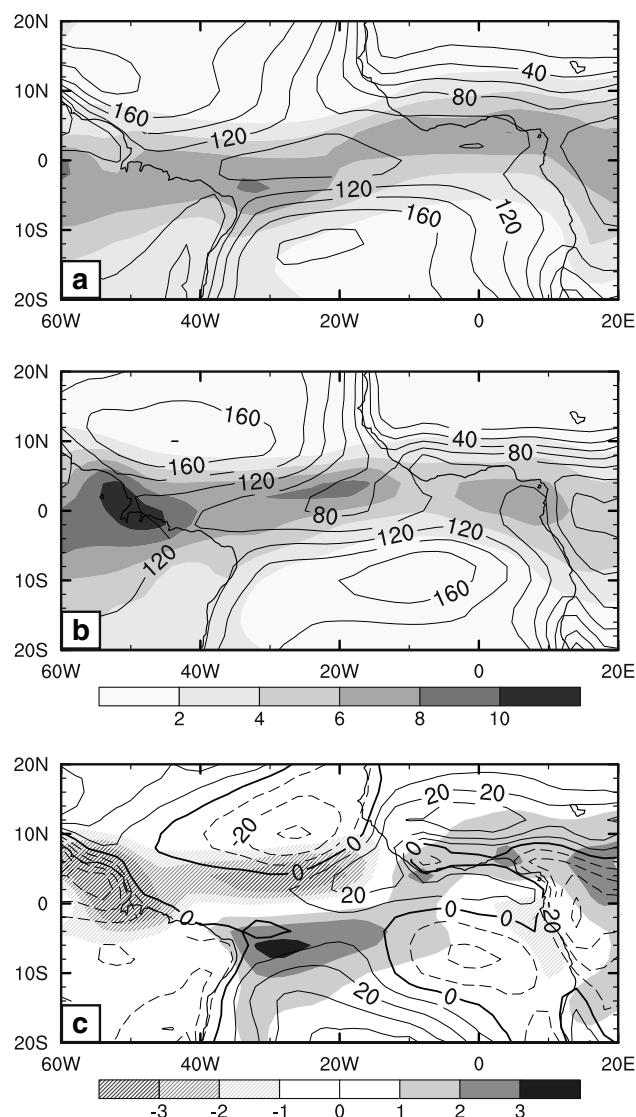


Fig. 13 Latent heat flux (W m^{-2} , contours) and precipitation (mm/day, shading) for **a** the AMIP ensemble mean, **b** NCEP reanalysis (latent heat flux) and CMAP (precipitation), and **c** the difference **a** minus **b**. In **c**, precipitation values above +1 mm/day and below –1 mm/day are indicated by *solid and cross-hatched shading*, respectively. Negative latent heat flux contours are *dashed*

improving precipitation over tropical South America and Africa has the potential to alleviate atmospheric circulation biases over the South Atlantic.

6 Summary and discussion

We have evaluated simulations by the IPCC AR4 coupled GCMs against observations. Our analysis shows that these models suffer major biases over the tropical Atlantic and adjacent continents. During MAM when the equatorial Atlantic is warm, the simulated ITCZ is erroneously

displaced south of the equator, with warm SST biases in the tropical Southeast Atlantic (meridional biases). Along the equator, models fail to develop the eastern cold tongue, with SST gradients opposite to observations in the central equatorial Atlantic (zonal biases). The largest SST errors along the equator are found in the eastern basin during JJA, the season when the cold tongue develops in observations. The largest surface wind errors, on the other hand, occur one season earlier in MAM and act to decelerate the prevailing easterlies on the equator. Without exception both surface wind errors and the southward shift of the ITCZ during MAM are already present in the atmospheric component of the CMIP models. These atmospheric model errors are amplified in CMIP runs by ocean–atmosphere interactions such as the Bjerknes and WES feedbacks. Specifically, westerly wind anomalies in MAM deepen the thermocline in the eastern equatorial Atlantic. Even though the wind biases decrease in JJA and the total winds are generally favorable for oceanic upwelling, the excessively deep thermocline does not allow an eastern cold tongue to develop in coupled GCMs. As a result of the failure to develop the cold tongue, the equatorial SST bias peaks during JJA.

Focusing on MAM, we further examine the AMIP simulations and trace the source of the equatorial westerly wind errors to a zonal dipole of precipitation errors on the adjacent continents: deficient precipitation over equatorial South America and excessive precipitation over tropical Africa. These rainfall errors drive a surface pressure gradient that decelerates the easterly winds. An important result useful for model developers is that errors of atmospheric GCMs during MAM are amplified in coupled simulations and lead to errors in the oceanic component that persist into the following season. Therefore, a realistic simulation of the MAM climate in atmospheric GCMs may hold the key to improving coupled model simulations. Specifically, our analysis indicates that the continental precipitation biases strongly affect, but are not significantly influenced by, climate biases over the Atlantic Ocean, which underlines the importance of examining biases over land.

While the present study points to errors in atmospheric GCMs and in representing terrestrial precipitation in particular, it does not rule out other possible sources of error in coupled models, such as the representation of oceanic upwelling and mixing (Hazeledger and Haarsma 2005; Large and Danabasoglu 2006). These processes likely also play a role in the pronounced warm bias of the southeastern Atlantic (Fig. 1), which, in turn, might contribute to the southward shift of the ITCZ in MAM as proposed by Huang et al. (2007). In our study, the southward ITCZ shift is limited to the western and central Atlantic for AMIP models (Fig. 4b) but extends all the way to the African coast for CMIP models (see Sect. 4). This suggests a local

effect of the southeastern SST bias on the ITCZ but the basic double ITCZ problem originates in the uncoupled AGCMs as illustrated by Fig. 4b. In any event, it is evident that many factors may contribute to coupled GCM biases in the tropics. Clearly much work is necessary to understand and reduce the errors that have long plagued coupled simulations in the tropical Atlantic.

Acknowledgments This study was supported by the NOAA CLIVAR Program and the Japan Agency for Marine–Earth Science and Technology through its sponsorship of the International Pacific Research Center. All the model output was downloaded from The IPCC Data Archive at Lawrence Livermore National Laboratory, which is supported by the Office of Science, U.S. Department of Energy. The authors would like to thank Justin Small and two anonymous reviewers for their helpful suggestions. IPRC publication #498.

References

- Biasutti M, Sobel AH, Kushnir Y (2006) AGCM precipitation biases in the tropical Atlantic. *J Clim* 19:935–958
- Breugem W-P, Hazeleger W, Haarsma RJ (2006) Multimodel study of tropical Atlantic variability and change. *Geophys Res Lett* 33. doi:[10.1029/2006GL027831](https://doi.org/10.1029/2006GL027831)
- Chang P, Coauthors (2006) Climate fluctuations of tropical coupled system—the role of ocean dynamics. *J Clim* 19:5122–5174
- Chang CY, Carton JA, Grodsky SA, Nigam S (2007) Seasonal climate of the tropical Atlantic sector in the NCAR community climate system model 3: error structure and probable causes of errors. *J Clim* 20:1053–1070
- Cohen JC, Silva Dias MA, Nobre CA (1995) Environmental conditions associated with Amazonian squall lines: a case study. *Mon Weather Rev* 123:3163–3174
- Conkright ME, Locarnini R, Garcia H, O'Brien T, Boyer TP, Stephens C, Antonov J (2002) World Ocean Atlas 2001, objective analyses, data statistics and figures, CD-ROM documentation, National Oceanographic Data Center. Silver Spring, MD
- Davey MK, Coauthors (2002) STOIC: a study of coupled model climatology and variability in tropical ocean regions. *Clim Dyn* 18:403–420
- Deser C, Capotondi A, Saravanan R, Phillips AS (2006) Tropical Pacific and Atlantic climate variability in CCSM3. *J Clim* 19:2451–2481
- de Szoeké SP, Xie S-P (2008) The tropical eastern Pacific seasonal cycle: assessment of errors and mechanisms in IPCC AR4 coupled ocean–atmosphere general circulation models. *J Clim* (in press)
- DeWitt DG (2005) Diagnosis of the tropical Atlantic near-equatorial SST bias in a directly coupled atmosphere–ocean general circulation model. *Geophys Res Lett* 32:L01703. doi:[10.1029/2004GL021707](https://doi.org/10.1029/2004GL021707)
- Dirmeyer PA, Koster RD, Guo Z (2006) Do global models properly represent the feedback between land and atmosphere? *J Hydro-meteor* 7:1177–1198
- Hagos SM, Cook KH (2005) Influence of Surface Processes over Africa on the Atlantic Marine ITCZ and South American Precipitation. *J Clim* 18:4993–5010
- Hazeledger W, Haarsma RJ (2005) Sensitivity of tropical Atlantic climate to mixing in a coupled ocean–atmosphere model. *Clim Dyn* 25:387–399

- Helber RW, Weisberg RH, Bonjean F, Johnson ES, Lagerloef GSE (2007) Satellite-derived surface current divergence in relation to tropical Atlantic SST and wind. *J Phys Oceanogr* 37:1357–1375
- Huang B, Schopf PS, Shukla J (2004) Intrinsic ocean–atmosphere variability of the tropical Atlantic Ocean. *J Clim* 17:2058–2077
- Huang B, Hu Z-Z, Jha B (2007) Evolution of model systematic errors in the tropical Atlantic basin from coupled climate hindcasts. *Clim Dyn* 28:661–682
- Kalnay E, Coauthors (1996) The NCEP/NCAR 40-year reanalysis project. *Bull Am Meteor Soc* 77:437–471
- Keenlyside NS, Latif M (2007) Understanding equatorial Atlantic interannual variability. *J Clim* 20:131–142
- Klein SA, Hartmann DL (1993) The seasonal cycle of low stratiform clouds. *J Clim* 6:1587–1606
- Kousky VE (1980) Diurnal rainfall variation in northeast Brazil. *Mon Weather Rev* 108:488–498
- Large WG, Danabasoglu G (2006) Attribution and impacts of upper-ocean biases in CCSM3. *J Clim* 19:2325–2346
- Ma CC, Mechoso CR, Robertson AW, Arakawa A (1996) Peruvian stratus clouds and the tropical pacific circulation: a coupled ocean–atmosphere GCM study. *J Clim* 9:1635–1645
- Mechoso CR, Robertson AW Coauthors (1995) The seasonal cycle over the tropical Pacific in general circulation models. *Mon Weather Rev* 123:2825–2835
- Meehl GA, Covey C, McAvaney B, Latif M, Stouffer RJ (2005) Overview of the coupled model intercomparison project. *Bull Am Meteor Soc* 86:89–93
- Mesinger F, Janjić ZI, Ničković S, Gavrilov D, Deaven DG (1988) The step-mountain coordinate: model description and performance for cases of Alpine lee cyclogenesis and for a case of an Appalachian redevelopment. *Mon Weather Rev* 116:1493–1518
- Mitchell TP, Wallace JM (1992) The annual cycle in equatorial convection and sea surface temperature. *J Clim* 5:1140–1156
- Okumura Y, Xie S-P (2004) Interaction of the Atlantic equatorial cold tongue and African monsoon. *J Clim* 17:3588–3601
- Okumura Y, Xie S-P (2006) Some overlooked features of tropical Atlantic climate leading to a new Nino-like phenomenon. *J Clim* 19:5859–5874
- Repelli CA, Nobre P (2004) Statistical prediction of sea surface temperature over the tropical Atlantic. *Int J Climatol* 24:45–55
- Richter I, Mechoso CR, Robertson AW (2008) What determines the position and intensity of the South Atlantic anticyclone in austral winter?—an AGCM study. *J Clim* 21:214–229
- Rickenbach TM (2004) Nocturnal cloud systems and the diurnal variation of clouds and rainfall in southwestern Amazonia. *Mon Weather Rev* 132:1201–1219
- Rossow WB, Schiffer RA (1999) Advances in understanding clouds from ISCCP. *Bull Am Meteor Soc* 80:2261–2287
- Rouault M, Florenchie P, Fauchereau N, Reason CJC (2003) South East tropical Atlantic warm events and southern African rainfall. *Geophys Res Lett* 30. doi:10.1029/2002GL014840
- Shannon LV, Boyd AJ, Brundrit GB, Taunton-Clark J (1986) On the existence of an El Niño type phenomenon in the Benguela system. *J Mar Res* 44:495–520
- Stockdale TN, Balmaseda MA, Vidard A (2006) Tropical Atlantic SST prediction with coupled ocean–atmosphere GCMs. *J Clim* 19:6047–6061
- Wang H, Fu R (2007) The influence of Amazon rainfall on the Atlantic ITCZ through convectively coupled Kelvin waves. *J Clim* 20:1188–1201
- Worley SJ, Woodruff SD, Reynolds RW, Lubker SJ, Lott N (2005) ICOADS Release 2.1 data and products. *Int J Climatol* 25:823–842
- Xie S-P (1996) Westward propagation of latitudinal asymmetry in a coupled ocean–atmosphere model. *J Atmos Sci* 53:3236–3250
- Xie P, Arkin PA (1997) Global precipitation: a 17-year monthly analysis based on gauge observations, satellite estimates, and numerical model outputs. *Bull Am Meteor Soc* 78:2539–2558
- Xie S-P, Carton JA (2004) Tropical Atlantic variability: patterns, mechanisms, and impacts. In: *Earth climate: the ocean–atmosphere interaction*. Geophys Monograph, vol 147. AGU, Washington DC, pp 121–142